S1 PWR SUBCHANNEL VOID DISTRIBUTION USING CFD METHODS

T.K.D. Hoang, P.K. Nguyen, V.H. Pham, X.L. Bui

School of Transportation Engineering, Hanoi University of Science and Technology

Contact E-mail Address: dung.hoangthikim@hust.edu.vn **or** dunghtk.dase@gmail.com

ABSTRACT Central (typical subchannel void distribution (S1) problem was carried out using CFD method. The steady-state void distribution benchmark based on the PWR (Pressurized Water Reactor) Subchannel and Bundle Test (PSBT) was simulated. The investigation has been carried out for three different test conditions (with respect to pressure, inlet fluid temperature, power and mass flow rate) from the PBST test matrix. The CFD calculation predicts the void distributions in S1 subchannel with different turbulent models. It is shown that the predicted averaged void fraction values have good agreement with measured cross section averaged values of the benchmark. The cross section void distribution illustrates the major effect of different turbulence models on the results.

1. INTRODUCTION

According to (Rubin, et al., 2010, Weis, et al. 2010, In, et al., 2010), NUPEC (Nuclear Power Engineering Corporation - Japan) PSBT benchmark consists of two phases with different exercises, where the first phase focuses on void distribution benchmark with four exercises. Therein, the first exercise is steady-state single subchannel benchmark with different geometries (S1, S2, S3 and S4). Fig. 1 shows the test section used for the typical center subchannel (S1) with the heated length of 1555mm and the measuring position of void fraction located at 1400mm elevation over the inlet. At cross section view, the diameter, pitch and gap of the rod are 9.5mm, 12.6mm and 3.1mm, respectively. Several runs were selected to experimental investigate, in which pressure varies from 50 to 169 kg/cm^2 (See Table 1).

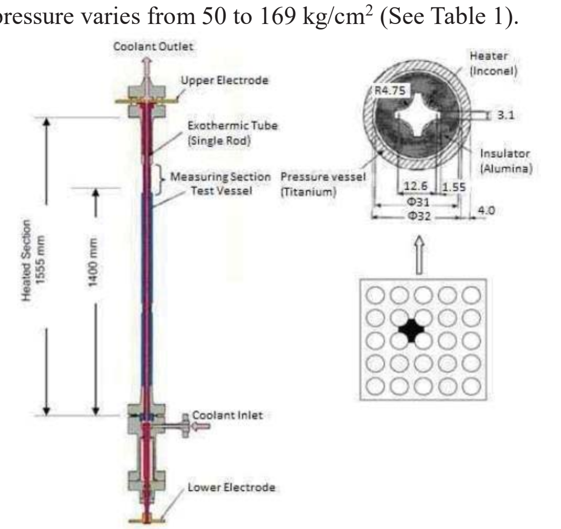

Fig.1 Test section for S1 subchannel void measurement

Table 1 Results of void fraction predicted by (Rubin, et al., 2010)

Run No	Pressure	Mass Flux	Power	Inlet Temperature	Exp.Void Fraction
	(kg/cm^2)	(10^6kg/m^{2}h)	(kW)	(°C)	
1.4324	100.1	5.02	60.1	238.9	0.157
1.4325	100.3	5.03	59.8	253.8	0.335
1.4326	100.1	5.02	60.1	268.8	0.531

Test conditions of the S1 subchannel tests were characterized by the four main parameters: pressure, inlet mass flux, thermal power and coolant inlet temperature, the latter corresponding to a certain liquid subcooling in correspondence to the saturation temperature for the given pressure level. A subset of 3 test conditions of total 43 different test conditions, which had been investigated in the NUPEC experiments, had been selected during the PSBT benchmark. The selected test conditions were summarized in Table 1.

The target of this study is to investigate the applicability of the CFX models to the PSBT test with help of ANSYS software. The numerical results is then compared with experimental results of (Rubin, et al., 2010) (Table 1).

2. NUMERICAL SETUP

2.1 Geometry and mesh

a. Geometry

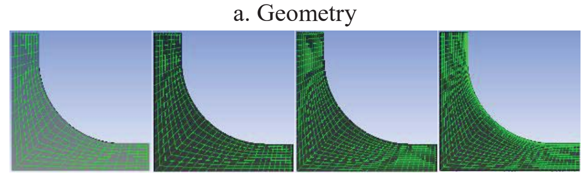

Mesh 1 Mesh 2 Mesh 3 Mesh 4

b. Mesh

Fig.2 Geometry and mesh

The S1 subchannel consists of a typical central subchannel of a fuel assembly where all four adjacent walls of heater rods are homogeneously heated by constant power over the total length of the heated part of the test section. The geometrical dimensions of the central subchannel are given in Figure 2. Due to the 90° symmetry, only 1/4th of the geometry will be simulated in the CFD simulations (Fig. 2a) (Hoang, et al., 2014, Hoang, et al., 2015).

Four different meshes are generated with various refinement factors in cross section as shown in Fig. 2b with helps of CFX-14.5 tool in ANSYS software. The four meshes consist of 58600, 85000, 124000 and 185600 elements, respectively.

2.2 Model setup

The two phase flow simulations were defined with water as continuous and steam as dispersed phase. The thermal energy heat transfer model was chosen for the liquid phase and the gas phase was defined to be isothermal at the corresponding saturation temperature.

Material properties for both vapor and liquid had been specified by defining material properties based on IAPWS-IF97 (International Association for the Properties of Water and Steam Industrial Formulation) water/water steam tables defined for the given range of temperature and pressure of the test cases.

The flow under investigation was described in the framework of the currently most conventional CFD approach to modeling gas-liquid two-phase flows with significant volume fractions of both phases – the Eulerian two-fluid model derived under the assumption of interpenetrating continua. Phase distribution resulted from solving the phase-specific continuity equations for volume fractions, and separate sets of momentum equations are solved for each phase, where buoyancy and interfacial momentum transfer was taken into account. Momentum transport equations were supplemented by turbulence model equations.

For the steam–water bubbly flow an energy equation was solved for liquid, while for the description of the nucleate subcooled boiling processes under consideration the vapour was assumed to be saturated at all time. The exchange of mass, momentum and heat between phases were modeled using the correspondent source terms in the phase-specific balance equations. For the dispersed bubbly flow assumed for the nucleate subcooled boiling processes the interfacial momentum transfer was modeled in terms of the Grace drag force due to the hydrodynamic resistance and the non-drag forces. In the present investigation non-drag forces with the exclusion of the virtual mass forces had been applied. The non-drag forces discussed here were: lift force, wall force and turbulent dispersion force.

Concerning the non-drag forces two different setups were tested. In the first set up, SST and k-ε turbulent model had been applied. Tomiyama's lift force correlation was added and Antal's correlation for wall lubrication force; Ishi & Zuber's correlation for drag force (Table 2). The turbulent dispersion force was modeled by Lopez de Bertodano.

In the second setup, only k-ε turbulent model had been applied. Other differences with setup 1 were lift force, drag force and mean bubble diameter. The lift force and drag force model were chose as 0.01 and 0.44 respectively.

The heat transportation between the heated wall and the fluid was occurred through various ways. On the wall area consisting of no bubble, heat was transferred directly to the subcooled liquid in the same mechanism of single phase flow. On the wall area that bubbles exist, heat was consumed by the generation of vapor. Furthermore, there was a liquid mixing mechanism due to the detachment of bubbles from the wall. The result was that cold liquid from the bulk of the flow was brought into contact with the hot wall which leads to additional cooling. This mechanism was termed quenching. The total heat flux was expressed as the sum of these contributions as:

$$Q_{Tot} = Q_C + Q_Q + Q_E \qquad (1)$$

where Q_C, Q_Q, Q_E denote the heat flux components due to single-phase turbulent convection, quenching, evaporation, respectively.

This was RPI (Rensselaer Polytechnic Institute) wall boiling model (Hoang, et al., 2014)

The mean bubble diameter was calculated locally as a linear function of liquid subcooling as Anglart (1997) proposed for setup 1:

$$d_B = \frac{d_{B,1}(T_{sub}-T_{sub,2})+d_{B,2}(T_{sub,1}-T_{sub})}{(T_{sub,1}-T_{sub,2})} \qquad (2)$$

For typical nuclear energy applications these authors proposed for subcooled nucleate boiling under PWR conditions (so, high pressure conditions) reference bubble diameters at the two reference subcooling conditions: $d_{B,1}$ = 0.1mm at $T_{sub,1}$ = 13.5K and $d_{B,2}$ =2mm at $T_{sub,2}$ = -5K.

For setup 2, the bubble departure diameter on the wall, d_w, was calculated by Tolubinski and Kostanchuk, 1970:

$$d_W = min\left(2d_{ref}exp\left(-\frac{\Delta T_{sub}}{\Delta T_{ref}}\right), d_{max}\right) \qquad (3)$$

In which, the parameters of the original model were dimensional:

d_{max} denoted maximum bubble departure diameter on the wall, d_{max}=1.4mm

d_{ref} denoted reference quantity of bubble departure diameter on the wall, d_{ref}=0.6mm

ΔT_{sub} refered to the local liquid subcooling, ΔT_{ref}=45K

Table 2 resumed the numerical setup of both gas phase and liquid subcooling.

Table 2 Multiphase flow setup

Water Steam	Setup 1	Setup 2
Turbulent model	SST & k-ε	k-ε
Lift force model	Tomiyama (2002)	0.01
Wall lubrication model	Antal (1991)	Antal (1991)
Drag force model	Ishi & Zuber (1981)	0.44
Turbulence dispersion force	Lopez	Lopez
Mean bubble diameter	Anglart (1997)	Tolubinskiy
Water	IAPWS-IF97	IAPWS-IF97

2.3 Boundary conditions

Boundary conditions were presented in Fig. 3. The walls were considered as adiabatic wall. In case of the heated walls a no-slip boundary condition was chosen for the liquid and a free-slip boundary condition for the gaseous phase. The wall contact model used the calculated volume fractions to evaluate the wetting of the wall surfaces.

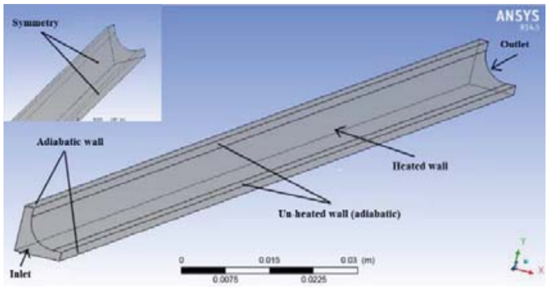

Fig.3 Boundary conditions

3. RESSULTS

In the subchannel experiments a narrow gamma-ray beam CT scanner was used to measure the subchannel averaged void fraction and a wide gamma-ray beam was used to measure the chordal averaged void fraction (Rubin, et al., 2010). Consequently for each subchannel test condition a cross sectional averaged steam volume fraction value and the cross sectional void distribution were provided.

3.1 Influence of mesh - SST turbulence model- Setup 1

The calculations for averaged cross section void fraction and radial void fraction distribution performed in four meshes for setup 1 showed no significant different in both averaged void fraction and radial void fraction distribution (Fig.4). There was a slightly increased averaged void fraction when increased quality of mesh from 58600 to 124000 elements. Between mesh 3 and mesh 4, there was no significant different in both averaged void fraction and radial void fraction distribution. Therefore, mesh 3 (124000 elements) was chose for other case.

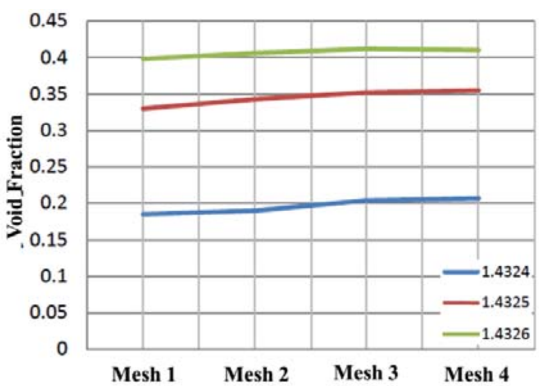

Fig.4 Influence of mesh – Setup 1

3.2 Influence of turbulence model

Fig. 5 showed the difference of void fracture between SST and k-ε turbulent model of setup 1 at position Z = 1.4m in the test case 1.4324. Void fracture of SST turbulence model and k-ε model setup 1 were respectively 0.220 and 0157. The difference was significant as 40%.

For SST model, maximum of void fraction was located in near heated wall and void fraction had a tendency to decline gradually towards center of subchannel. (Fig. 6a).

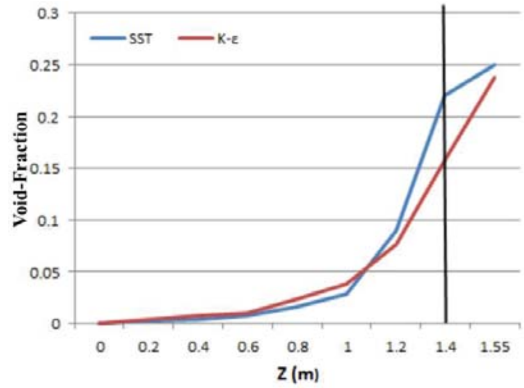

Fig. 5 Influence of turbulent model – Setup 1

Run 1.4324 Run 1.4325 Run 1.4326

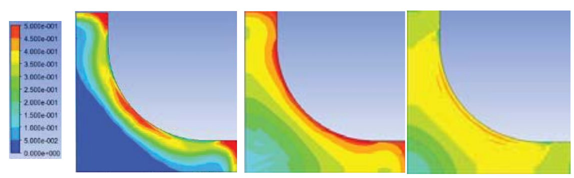

a. SST – Setup 1

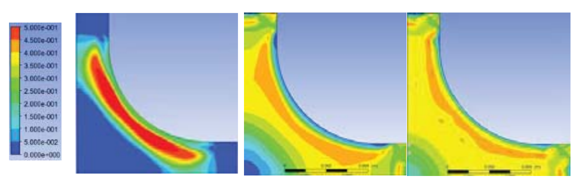

b. k-ε – Setup 1

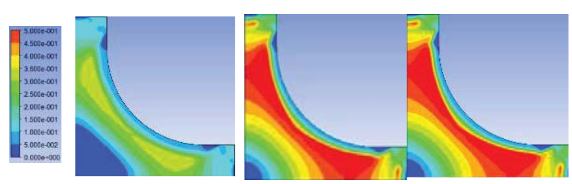

c. k-ε – Setup 2

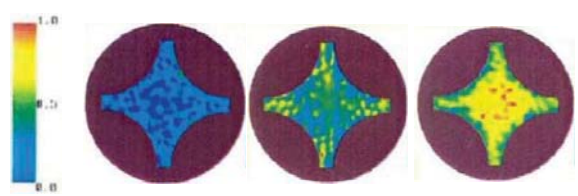

d. Experimental results

Fig. 6 Void fracture distributions

For k-ε model setup 1, there was a larger volume of steam concentrated near the heated wall while, in the center position of subchannel, there was completely without the presence of steam (Fig. 6b).

With the setup 2 (k-ε model), there existed a thin strip of no steam heat damage near heated wall as well as at the center subchannel position. Meanwhile, steam was evenly distributed in the corner in the center of subchannel (Fig. 6c).

With increasing of inlet temperature through three tests, maximum void fraction was shifted from the corner zones towards core region (Fig. 6).

In comparison with experimental results, the void fracture distribution of k-ε setup 2 was more closely to the experimental value (Fig.6d, Table 3). Thus, the turbulence model had strong impact to the results of model simulations.

Table 3 Averaged void fracture

Run case	EXP	NUM			Error (%)		
		SST Setup1	k-ε Setup1	k-ε Setup2	SST Setup1	k-ε Setup1	k-ε Setup2
1.4324	0.157	0.204	0.155	0.162	29.94	1.27	3.18
1.4325	0.335	0.382	0.31	0.334	14.03	7.46	0.30
1.4326	0.531	0.412	0.426	0.517	22.41	19.77	2.64

EXP: Experimental results *NUM: Numerical results*

Overall, the numerical results were fairly precise and differed from the experimental results by 14-30%, 1-20% and 0.3-3% for SST, k-ε setup 1 and k-ε setup 2 turbulent model respectively, with respects to cross sectional averaged void fraction at the measurement plane.

`

CONCLUSION

The presented CFD investigations using ANSYS-CFX 14.5 was used to calculate the averaged void fraction and predict the void distribution in the PSBT S1 PWR Subchannel. There was a small influence of mesh from 58600 to 185600 elements to the void fracture distribution and averaged void fracture. However, the void fracture distribution depended greatly on turbulent models. The relative error was about 0.3 to 30% between numerical results and experimental results.

Although, further research is required to improve the accuracy of the CFD model by adjusting suitable calibrated correlations. The void distribution has been shown to depend greatly on the turbulence models. In order to obtain more reliable results, much more detailed experimental investigations seem to be necessary.

REFERENCES

Rubin, A., Schoedel, A., Avramova, M., Utsuno, H., Baojorek, S., and Valaxquez-Lozada, A., OECD/NRC Benchmark Based on NUPEC PWR Subchannel and Bundle Tests (PSBT), Volume I: Experimental Database and Final Problem Specifications, *US NRC/OECD Nuclear Energy Agency*, November 2010, pp. 12-22.

Weis, J., Papukchiev, A., and Scheuerer, M., CFD analysis of boiling flow in PWR subchannel geometry of the OECD/NRC PSBT benchmark exercise I-1, *The 14th International Topical Meeting on Nuclear Reactor Thermalhydraulics*, 2010.

In, W.K., Shin, C.H., and Chun, T.H., CFD application to PWR subchannel void distribution benchmark, *The 14th International Topical Meeting on Nuclear Reactor Thermalhydraulics*, 2010

Hoang, M.G., and Nguyen, P.K., Numerical investigation of departure bubble diameter of wall boiling model in PWR subchannel, *The 7th AUN/SEED-Net Regional Conference in Mechanical and Manufacturing Engineering*, Vietnam, 2014

Hoang, M.G., Phung, D.T., Nguyen, P.K., and Hoang, T.K.D., Modelling of the PWR subchannel void distribution based on CFD approach, The 3rd AUN/SEED-Net Regional Conference on Natural Disaster: Building Resilient Communities, Philippines, 2015

Antal, S.P., Lahey, R.T., and Flaherty, J.E., Analysis of phase distribution in fully developed laminar bubbly two-phase flow, *Int. J.l of Multiphase Flow*, vol. 7, pp. 635-652, 1991.

Anglart, H., Nylund, O., Kurul, N., and Podowski, M.Z., CFD prediction of flow and phase distribution in fuel assemblies with spacers, NURETH-7, 1995 Saratoga Spring, New York, *Nuclear Engineering and Design*, Vol.177, pp.215-288, 1997.

Tolubinski, V. I. and Kostanchuk, D.M., Vapor bubbles growth rate and heat transfer intensity at subcooled water boiling, *Proceeedings of the 4th International Heat Transfer Conference*, Paris, 1970

Nguyen Phu Khanh received the B.E. (2000) in Aeronautic from Hanoi University of Science and Technology - Vietnam, M.E. (2001) in Aeronautic from National University of Mechanical and Aeronautics Engineering (ENSMA) University – France and D.E. (2006) degrees in Aeronautic from ENSMA University – France. He is an Associate Professor, Department of Aeronautic and Space Engineering, Hanoi university of Science and Technology – Vietnam. His current interests include: Fluid Mechanics; Energy and Combustion; Nuclear Engineering; Simulation Technology

Hoang Thi Kim Dung received the B.E. (2004) in Mechanical and Aeronautical Engineering from Hanoi University of Science and Technology - Vietnam, M.E. (2005) in Aeronautical Engineering, Fluid, Acoustic and Energy from National University of Mechanical and Aeronautics Engineering (ENSMA) University – France and D.E. (2009) degrees in Aeronautical Engineering, thermal-Aerodynamics from ENSMA University – France.

She is a Doctor Lecturer, Department of Aeronautic and Space Engineering, Hanoi university of Science and Technology – Vietnam. Her current interests include: Fluid Mechanics; Energy and Combustion; Nuclear Engineering; Simulation Technology.